THIRD QUARTERLY REPORT ON THE DEVELOPMENT OF MEDICAL AND BIOLOGICAL SEMICONDUCTOR DETECTORS

28 p.

N63 18369
CODE-1

OTS PRICE

XEROX $ [redacted]
MICROFILM $ [redacted]

Submitted by

SOLID STATE RADIATIONS, INC.,
2261 South Carmelina Avenue
Los Angeles 64, California

8148504

April 30, 1963

This work is supported by the National Aeronautics & Space Administration, Manned Spacecraft Center, General Research Procurement Office, Houston 1, Texas, under Contract NASw-415

PROJECT LEADER: F. P. Ziemba

WORK DONE BY: J. Friederichs, J. Moross, J. Berdaner, et al

CR-50,521

TABLE OF CONTENTS

18369

SUMMARY

During the period covered by this report the major effort was placed on the fabrication and evaluation of 3mm diameter medical probes suitable for invivo measurements. Specifically, the fabrication process for these detectors was finalized and a number of these detectors were fabricated. After the mechanical and electrical characteristics of the devices were obtained, the units were evaluated in various nuclear environments.

This report contains a summary of the final fabrication procedure used as well as the results of the evaluation of these detectors carried out at SSR facilities. The detectors were evaluated with alpha particles, betas and Co^{60} gammas. In particular, the data obtained with P^{32} solutions demonstrated that invivo measurements at typical medical dosage levels could be carried out quite easily.

I. FABRICATION PROCESS FOR 3mm DIAMETER INVIVO MEDICAL PROBE

The various steps used in the fabrication of the 3mm diameter medical probe are shown schematically in Figures 1 through 7. Figure 8 shows an assembly drawing and Figure 9 shows the final form of the detector probe. The sequence of steps in the process is described below:

1. The medical probes are fabricated from p-type float zone silicon having a resistivity in the 3500 to 4500 ohm-cm range. The crystals have a 1-1-1 orientation and are 3/4" to 7/8" in diameter.

2. The crystal is mounted on a ceramic block with wax and sliced, the slices being approximately 1/4" thick. The slicing is done with a high speed diamond impregnated saw.

3. A planetary lapper is used to lap both sides of the wafers, whereupon some of the damage introduced by the saw is removed. The units are then mounted in preparation for the ultrasonic dicing operation.

4. Using a specially designed dicing tool on the ultrasonic impact grinder, nine cylindrical shaped units are diced from each of the wafers.

5. The cylindrical units are now placed upon a rotating fixture, whereupon the nose of the unit is shaped using various grades of emory cloth. The unit is now shaped like a bullet and is ready for the various diffusion steps.

6. The first diffusion is a rather deep one using phosphorous as the doping material. The diffusion process is carried out for sixteen hours at 1200°C. The diffusion depth is calculated to be approximately 50 microns. This deep diffused layer is used as the base for a soldering process described later on. The diffusion depth was measured by means of the energy loss by 6 Mev α particles in the "window" or diffused layer. Results of these measurements were in agreement with the calculated diffusion depth. These measurements were also corroborated by sectioning and copper plating the phosphorous (n-type) doped layer.

7. Since the thick diffused layer is undesirable on the nose

of the unit which is exposed to the radiation, a wax mask is applied to the sides and rear of the unit, whereupon the thick diffused layer on the nose is removed by etching.

8. After removal of the wax mask, a second phosphorous diffusion is carried out at a temperature of 1050°C. This diffusion cycle obtains a diffused layer of approximately 1 micron on the nose of the bullet shaped detector. This end of the unit is exposed to the radiation and presents a thin window which is necessary for heavy charged particle detection (such as α particles).

9. The rear of the bullet is now removed by lapping in preparation for the application of the aluminum alloy (p-type) contact.

10. A small diameter hole is ultrasonically cut axially from the back of the bullet. The combination of the phosphorous diffused surface and the aluminum alloy layer within the hole produce very nearly cylindrical geometry in the final detector.

11. The unit is now masked with wax on both the nose and the back, exposing the sides which have the deep phosphorous diffused layer. This step is in preparation for the nickel plating which is deposited along the sides of the bullet.

12. Electroless nickel is plated along the side of the bullet for soldering to the case.

13. Both the aluminum alloy back contact and the sintering of the nickel are carried out at the same time. First, an aluminum slug is placed into the ultrasonically diced hole at the back of the unit and a 16 mil diameter wire is inserted into the hole.

14. The bullets are set into a special fixture and the nickel wire is weighted down to insure adequate alloying during the heating cycle. At a temperature of 800°C, the aluminum is alloyed into the back, making the p^+ contact and the nickel is sintered into the sides of the unit to obtain greater adherence of the nickel to the silicon.

15. After the alloying and sintering step, the nose and back of the bullet are again wax masked in preparation for a second

nickel plating.

16. A second plate of electroless nickel is applied to the sides of the probe.

17. The nickel plated area is then dipped into molten tin as a pre-tinning operation.

18. In order to clean up the junction, all of the sides of the bullet are wax masked and the back end of the bullet is etched to produce a junction with high voltage and low leakage characteristics.

19. The unit is now ready to be soldered into the top part of the case. This step is done by dipping the nose of the bullet into molten tin. Since the tin does not wet the nose of the bullet, only soldering occurs along the pre-tinned region, thereby obtaining a hermetically sealed joint between the case top part and the silicon bullet.

20. The subassembly consisting of the bullet and the top part of the case is now tested for leaks by inserting the case into a tygon tube through which nitrogen under 25 lbs. of pressure is introduced. The unit being submerged in methanol to observe any bubbles which might be formed due to leakage of the hydrogen through the solder seal.

21. After the unit has been shown to be tight, the junction is coated with Dow Corning Silgard No. 183 and cured at 125°C for sixteen hours.

22. Electrical tests are now carried out on the subassembly in order to determine the characteristics of the diode. The unit is tested for light sensitivity and the current voltage characteristic is observed on a curve-tracer. The reverse characteristic must show low leakage and high voltage breakdown in order to be a suitable device. The forward characteristic is also examined since the properties of the contacts to the silicon may be determined from its shape.

23. The assembly of the back end of the probe is now carried out. Basically, the detector is composed of (a) the bullet shaped silicon which is soldered to the top part of the case and (b) a miniature coaxial cable which is hermetically sealed to the back part of the case.

24. The coaxial cable is soldered to the back part of the case. The braided shield is soldered to the case while the insulated central wire is exposed. This central wire will later be attached to the wire protruding from the hole in the back of the silicon.

25. A small extension to the back part of the case is then soldered in place. This extension to the back part of the case is referred to in the figures as the center part of the case and its function is to hold an insulated ring in place through which the inner conductor of the coaxial cable is threaded.

26. The region between the center ring washer and the back part of the case is filled with epoxy which is cured at a room temperature for twelve hours. This epoxy joint insures a rugged connection of the central wire to the cable and prevents any moisture from entering the detector portion of the case through the coaxial cable.

27. The subassembly composed of the cable and back part of the case is now tested for mechanical leaks using techniques described before.

28. The unit is now ready for final assembly. Using a special fixture, both ends of the wire are pre-tinned and the two wires are joined together using a teflon tube as insulation from the sides of the case. The two subassemblies are joined together and soldered using tin.

29. The outside shell of the probe is now cleaned and the excess tin from the soldering operation is removed.

30. After protecting the silicon nose with silastic rubber, the case walls are pre-plated with .15 to .20 mils of copper and flashed with a thin film of gold. The gold layer is also of the same order of thickness as the copper plate layer.

31. The complete assembly is leak tested by dipping into boiling xylene. An examination of the current voltage characteristics of the unit before and after the boiling process demonstrates the tightness of the unit.

32. The unit is completed and is ready for further electrical and nuclear tests.

II. ELECTRICAL AND NUCLEAR CHARACTERISTICS OF THE 3mm DIAMETER INVIVO MEDICAL PROBE

A block diagram of the electronic system used for the evaluation of the medical probe detectors is shown schematically in Figure 10. The system is composed of a vacuum chamber where the detector is placed, a charge sensitive preamplifier, followed by a variable integrating and differentiating circuit. The output of the amplifier is obtained on either an AC voltmeter which reads the RMS noise level, an oscilloscope, or a multichannel pulse height analyzer for spectral measurements. A step function pulse generator injects charge into the preamplifier to monitor any gain changes in the system. This system is used for determining the noise properties of the detector as well as determining the response of the probes to short range particles such as α's. A slightly different system is used when determining the response of the probes to β's and γ's. Before presenting the noise measurements on the detectors, it is perhaps advisable to review the problem of signal and noise in semiconductor-amplifier systems.

The calculation of an individual noise source to the noise output of the detector-amplifier system involves the integration over frequency of the product of the noise $n(\omega)$ and amplifier gain $g(\omega)$. The gain $g(\omega)$ depends upon the pulse shaping network of the amplifier. The simplest network, which is one of the best from a noise viewpoint, is an amplifier containing one R_1C_1 integrator and one R_2C_2 differentiator, the two time constants being equal. For such an amplifier $g(\omega) = \omega\tau/(1+\omega^2\tau^2)$, where $\tau = R_1C_1 = R_2C_2$ and $\omega = 2\pi f$.

If a nuclear particle deposits a charge Q onto the input capacitance C in a time which is short compared to τ, the amplifier will pass an exponentially rising and falling pulse with a maximum height equal to 0.37 Q/C independent of τ. The discussions which follow refer to such an amplifier.

Studies of the various noise sources in a detector-amplifier system indicate that tube shot noise and the detector leakage noise are the two most important noise sources in a well designed system. The equivalent RMS charge, which produces a pulse height equal to the RMS shot noise level at the amplifier input, given by $Q^2_{rms} = (10\ kT\ C^2)\ /\ (g_m\tau)$, where k is the Boltzman constant, T the absolute temperature, g_m is the mutual conductance of the input tube, τ is the amplifier time constant (with equal integrating and differentiating amplifier time constants), and C is the total input capacitance of the amplifier including the detector. The noise due to detector leakage current can be shown to be given by $Q^2_{rms} = 2eI_d\tau$, where e is the electronic charge and I_d is the leakage current in the detector.

The energy calibration of the electronic system shown in Figure 10 is obtained using the following procedure: The mercury relay type step function generator is used to transfer a fixed amount of charge into the charge sensitive preamplifier with the detector in place, and a spectrum of the signal generator as well as a Cs^{137} β source is obtained with a 256 channel pulse height analyzer. The 625 Kev internal conversion line of Cs^{137} is used to calibrate the analyzer and the full-width-at-half-maximum (FWHM) of the gaussian shaped spectrum of the pulse generator is measured. After removal of the source and pulse generator, a measurement of the noise is made on the wide band AC voltmeter, thereby calibrating the meter to read FWHM noise in Kev directly. All pulse shaping is done in the pulse integration and differentiation circuit. This circuit allows the variation of the amplifier time constants from 0.1 microsecond to 10 microseconds, the two time constants (integration and differentiation) being kept equal. Since the tube shot noise varies as $C/\tau^{1/2}$ and the detector leakage current noise varies as $(I_d\tau)^{1/2}$, it follows that the noise meter reading (FWHM in Kev) versus the amplifier time constant τ, clearly shows the contributions to each of the noise sources.

Figure 11 shows the FWHM noise in Kev versus the amplifier time constant with various standard capacitors plugged into the detector socket. The lowest curve gives the FWHM versus τ with the detector chamber disconnected from the amplifier input. The amplifier input under these conditions has an estimated capacitance of 15pf, including the charge feedback capacitor. The lowest curve labeled 0pf is for the amplifier when attached to the detector chamber, the chamber adds about an additional 20pf to the amplifier input. Curves marked 20pf, 100pf, 150pf and 200pf were obtained by plugging standard capacitors into the detector socket. These various curves are carried over to subsequent figures for comparison purposes as dashed curves.

The FWHM noise in Kev versus the amplifier time constant in microseconds are shown in Figures 12 and 13. Data at several operating voltages are given. The data for detector #MP-3001 (shown in Figure 12) demonstrate that the noise at short amplifier time constants is controlled by the shot noise in the input tube circuit. The rather large detector capacitance due to the coaxial cable is the source of this noise. At longer time constants, the system noise is controlled by the leakage current in the detector and successively higher noise values are obtained as the detector bias (and, therefore, the detector leakage current) is increased. The data for probe #MP3002 shown in Figure 13 are similar, although this particular unit is somewhat leakier and shows somewhat higher noise. The capacitance of probe #MP3002 is somewhat higher due to the longer length of cable used with this unit. One generally uses amplifiers with time constants at about 1 microsecond in order to obtain a compromise between speed and signal-to-noise ratio. Using much shorter amplifier time constants will obtain lower noise figures; however, the pulse shape is generally not suitable for the following electronic system which may be either count rate meter type circuitry when activity measurements are being made, or a pulse height analyzer when spectral measurements are being determined. The response of the medical probe detector to α particles is shown in Figures 14 and 15. These data were taken in order to determine the usefulness of the probe as an α particle detector as well as to examine the collection efficiency of the detector itself. Both figures show spectrum of α particles due to a Pb^{212} source which has a 6.04 and an 8.78 Mev α particle. The top spectrum in each of the figures is obtained with a standard NPS detector for comparison with the response obtained with the medical probe detectors shown in the lower three spectra. The line obtained from a pulse generator is also included to determine any gain shifts in the system due to change in the detector from the standard detector to the medical probe unit. The data shown in Figure 14 were obtained with the α particle striking the side of the detector, while the data of Figure 15 were obtained with the α striking the nose of the bullet shaped unit. In each case, the data were taken with the detector operating in the range of 25 volts to 100 volts bias. Although the two α lines are clearly visible in each of the two orientations, it is observed that the resolution is somewhat degraded. The degradation is attributed to the fact that α particles entering both the side and the front of the detector pass through different window thicknesses due to the angle at which they strike the detector. The data do, however, demonstrate that the probe is quite useful for the detection and even the spectroscopy of α particles. Excellent signal-to-noise ratios are obtained when using these detectors as α particle detectors and the low background of the semiconductor detector makes it most suitable for α particle detection in medical applications. Experience with these units has shown that α particles with energies above a few hundred Kev may be detected with essentially no background.

Data showing the response of the medical probe detectors to P^{32} β's in solution are summarized in Table I. The electronic system used to obtain these data is shown in Figure 16. The system is composed of an SSR Model 102-A charge sensitive preamplifier which is powered by a Model 202 power supply. A step function pulse generator is used to inject the charge into the preamplifier for gain monitoring purposes. The medical probe detector is attached to the preamplifier and inserted into a solution containing the P^{32} or a container of pure water which is used to obtain background measurements. The P^{32} in water solution was diluted to obtain a concentration of .014 microcuries/ml. Referring to Table I, the first column gives the reverse bias at which the detector was operated, the second column gives the counting rate per minute while the detector is inserted into the pure water. These are essentially the background counting rates for the system. The third column gives the counting rate per minute when the probe is inserted into the P^{32} solution. The fourth column gives the counting rate after the unit has been decontaminated and is placed back into the water solution. Data at 60 volts bias show that the background counting rate is 3 or 4 counts per minute, while the counting rate in the P^{32} solution was 101 counts per minute. At a bias of 20 volts the unit showed only one or two counts per minute background, while a counting rate of 33 counts per minute was obtained in the P^{32} solution. These data are typical of several medical probes which were evaluated in the β solution. These data demonstrate that the detector is quite suitable for the detection of P^{32} β's in invivo measurements.

The medical probe detectors are currently being evaluated with Co^{60} γ's to determine the sensitivity of the detectors to high energy γ's. A preliminary analysis of these data have shown that the device is capable of γ detection down to lowest levels which are used in normal medical applications. A complete report of γ measurements will be included in the final report.

TABLE NO. 1

COUNTING DATA FOR MEDICAL PROBE DETECTOR #3D-2
SOURCE: P^{32} IN H_2O SOLUTION: 0.0140μc/mℓ

REVERSE BIAS (V)	COUNTS/MIN* H_2O BLANK	COUNTS/MIN* P^{32}	COUNTS/MIN* H_2O AFTER DECONTAMINATION
60	3	101	4
20	1	33	—

* — ONLY COUNTS IN CHANNELS 10 TO 256 WERE CONSIDERED

PROCESS: 3 mm PROBE

STEP #

(1) 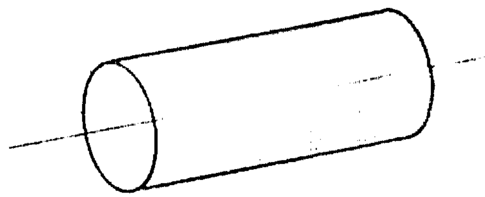

SILICON INGOT
"P" TYPE, 3500 TO 4500 Ω/cm
ORIENTATION 1-1-1
3/4 - 7/8 DIA

(2) 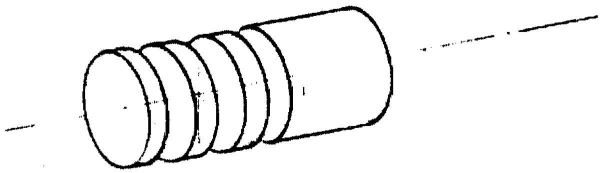

SLICE INGOT TO .250 ~ 6 1/2 mm SLICES

(3) 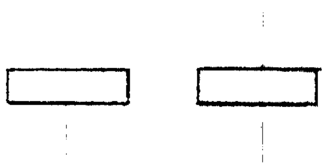

LAP SLICES ON BOTH SIDES

(4) 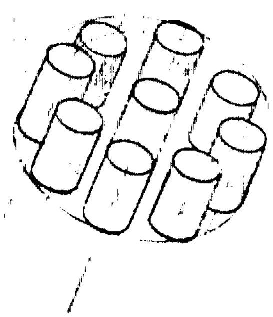

ULTRASONIC DICE SLICES INTO CYLINDRICAL PELLETS (USE SPECIAL MADE DICING TOOL ON IMPACT GRINDER)

(5) 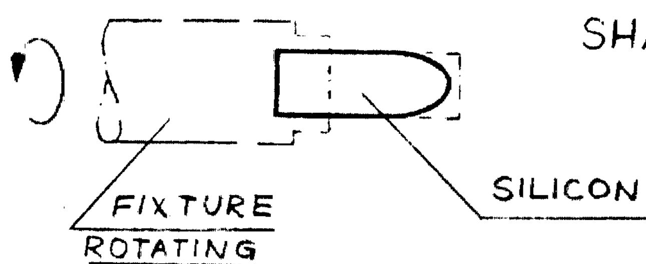

SHAPE "NOSE"

FIG. 1

PROCESS: 3 mm PROBE

STEP #

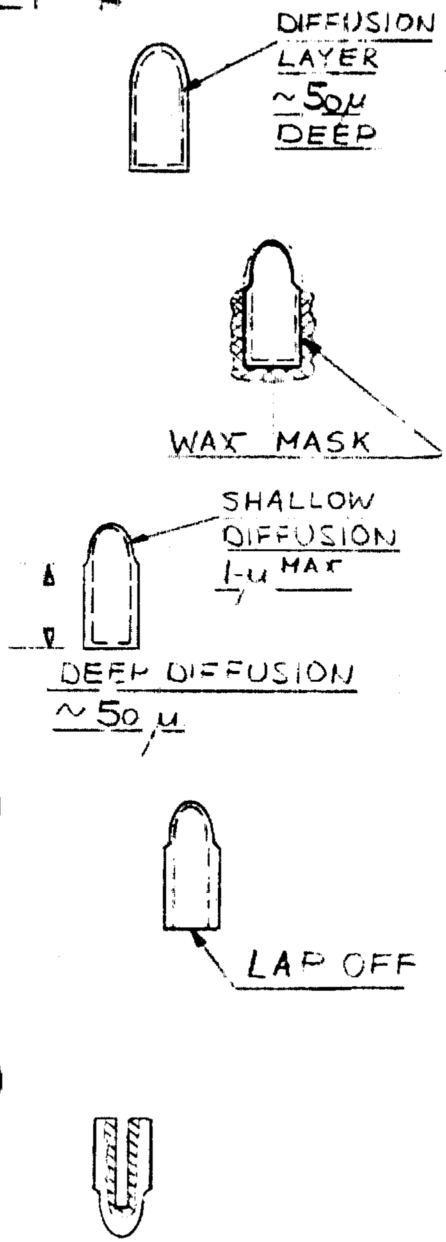

(6) PHOSPHOROUS
-FIRST-DIFFUSION (DEEP)
16^h-1200°C - GASFLOW: 6-ft^3 h-NITROGEN

(7) MASK BACK OF CRYSTAL AND ETCH "NOSE"
(ETCH OFF DIFFUSIONLAYER ON NOSE)

(8) PHOSPHOROUS
-SECOND-DIFFUSION, 1050°C, PROGRAM COOLING
GASFLOW: 6-ft^3 h-NITROGEN

(9) LAP OFF BACK OF CRYSTAL

(10) ULTRASONIC DICE HOLE (FOR BACKCONTACT)
IN SILICON
USE SPECIAL TOOL

FIG. 2

PROCESS 3mm PROBE

STEP #

(11)

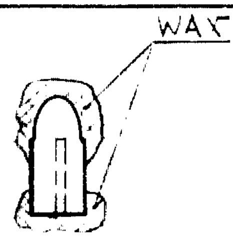

MASK CRYSTAL FOR ELECTROLESS NICKEL PLATING

(12)

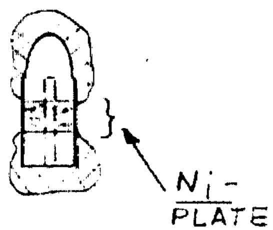

PLATE ELECTROLESS NICKEL

(13)

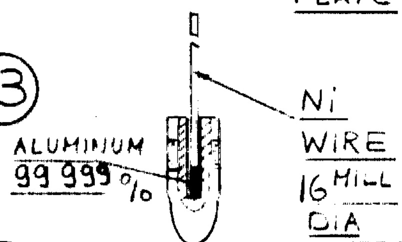

ATTACH WIRE TO BACK OF CRYSTAL

(14)

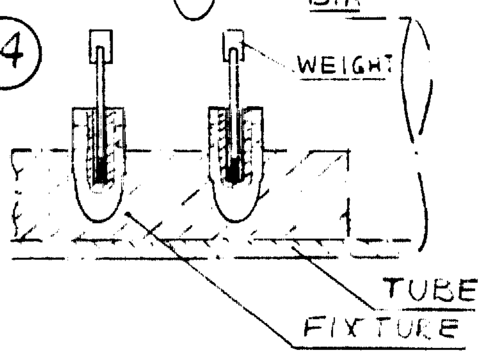

ALLOY ALUMINUM AND WIRE
AND SINTER NICKEL
USE TUBE FURNACE, 800°C IN NITROGEN

(15)

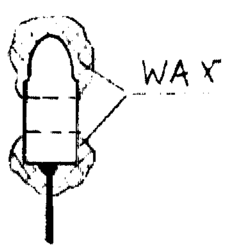

REMASK CRYSTAL FOR SECOND N_i-PLATE

FIG. 3

PROCESS 3mm PROBE

STEP #

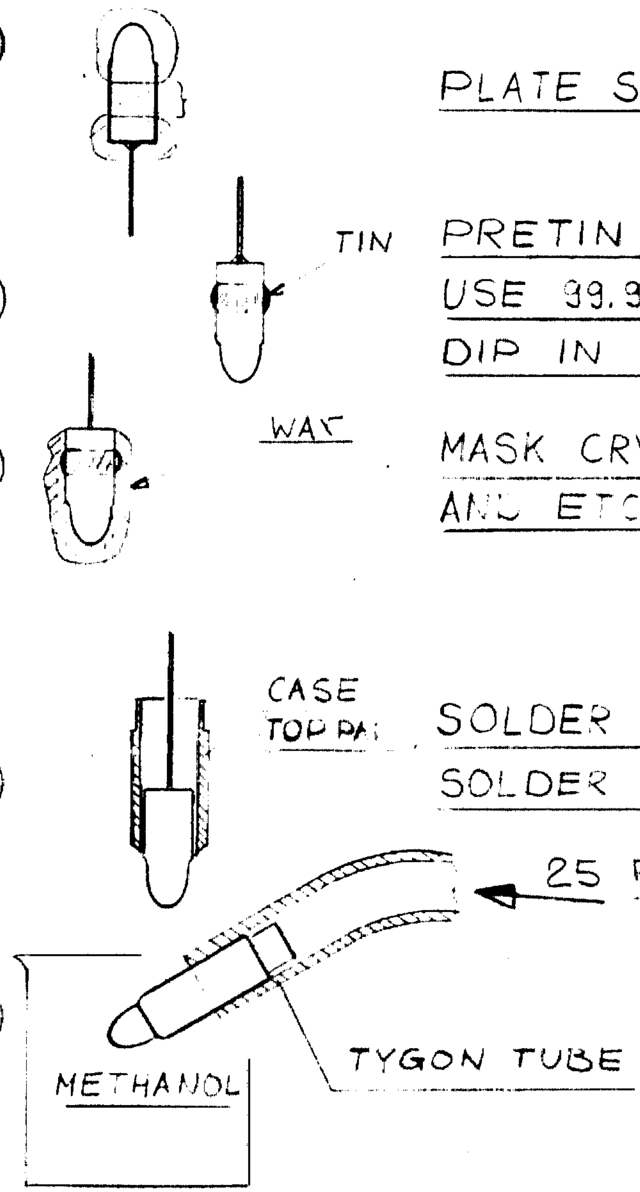

(16) PLATE SECOND LAYER OF ELECTROLESS NICKEL

(17) PRETIN N_i-PLATED AREA, FLUX WITH HYDRAZINE
USE 99.99 TIN
DIP IN MOLTEN TIN

(18) MASK CRYSTAL FOR BACK-(MESA) ETCHING
AND ETCH (4-PARTS HF, 6-PARTS NITRIC, 3-PARTS ACETIC, 3-PARTS PHOSPHORIC)

(19) SOLDER CRYSTAL TO CASE (TOP PART OF CASE)
SOLDER BY DIPPING INTO MOLTEN TIN

(20) TEST SUBASS'LY FOR MECH. LEAKS
APPLY 25 PSI. NITROGEN
IMMERSE SUBASS'LY INTO METHANOL

FIG. 4

PROCESS 3mm PROBE

STEP #

(21)

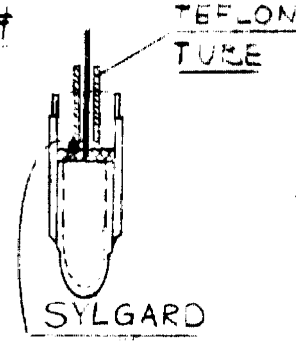

PROTECT JUNCTION WITH SYLGARD # 183
AND CURE AT 125°C FOR 16h IN CURINGOVEN
SLIP TEFLON TUBE OVER N_i-WIRE

(22)

CONDUCT ELECTRICAL PRE-TESTS
AND COLLECT DATA

BACKENDASS'LY OF PROBE

(23)

PREPARE CABLE (MICRODOT # 75-3925
75 Ω, CONNECTOR MOUNTED # 32-67)

(24)

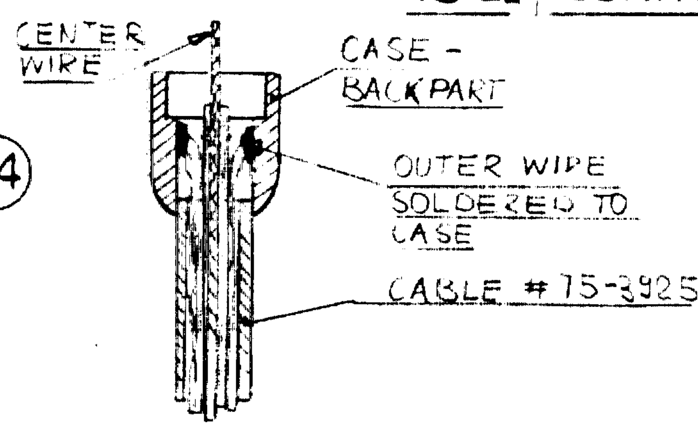

SOLDER CABLE TO CASE (BACKPART)
PRETIN I.D. OF CASE
USE 99.999 TIN
USE SPECIAL FIXTURE

FIG. 5

PROCESS 3 mm PROBE

STEP #

(25)

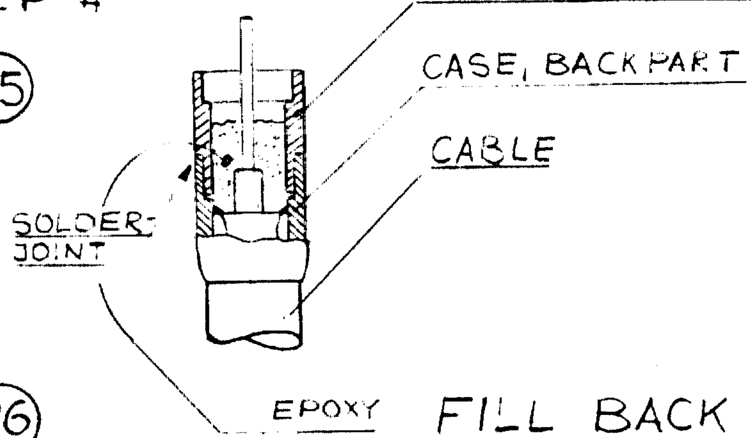

SOLDER CENTERPART OF CASE TO BACKPART OF CASE
USE TIN 99.999 %
USE SPECIAL FIXTURE

(26) FILL BACK OF SUBASS'LY WITH EPOXY AND CURE AT ROOMTEMP. FOR 12^h

(27) TEST SUBASS'LY FOR MECH. LEAKS
USE TECHNIQUE AS SHOWN IN STEP # (20)

(28) FINAL ASS'LY OF PROBE

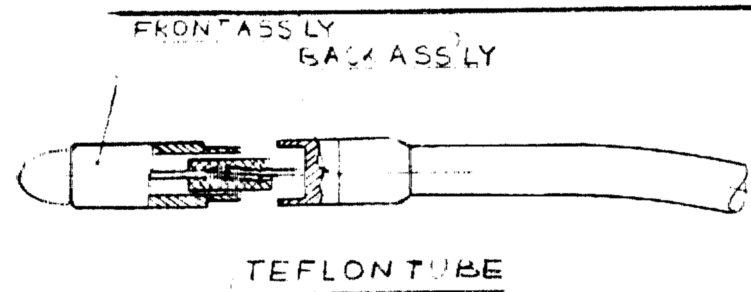

a) USE SPEC. FIXTURE
b) PRETIN BOTH WIRES
c) MAKE CONTACT BY JOINING WIRES
d) USE TEFLON TUBE
e) SOLDER SUBASS'LIES, USE 99.999 TIN

FIG. 6

PROCESS 3mm PROBE

STEP #	
29	CLEAN OUTSIDE SHELL OF PROBE REMOVE EXCESS OF TIN
30	PLATE PROBE a) PROTECT SILICON NOSE WITH SILICON RUBBER b) PREPLATE WITH Cu. .00015 TO .00020 c) FLASH WITH Au. .000020 TO .000025 (24-KARAT GOLD)
31	CONDUCT FINAL LEAKTEST DIP UNIT IN HOT (BOILING) XYLENE
32	FORWARD UNIT TO EVALUATION DEPT. FOR FURTHER TESTING

FIG. 7

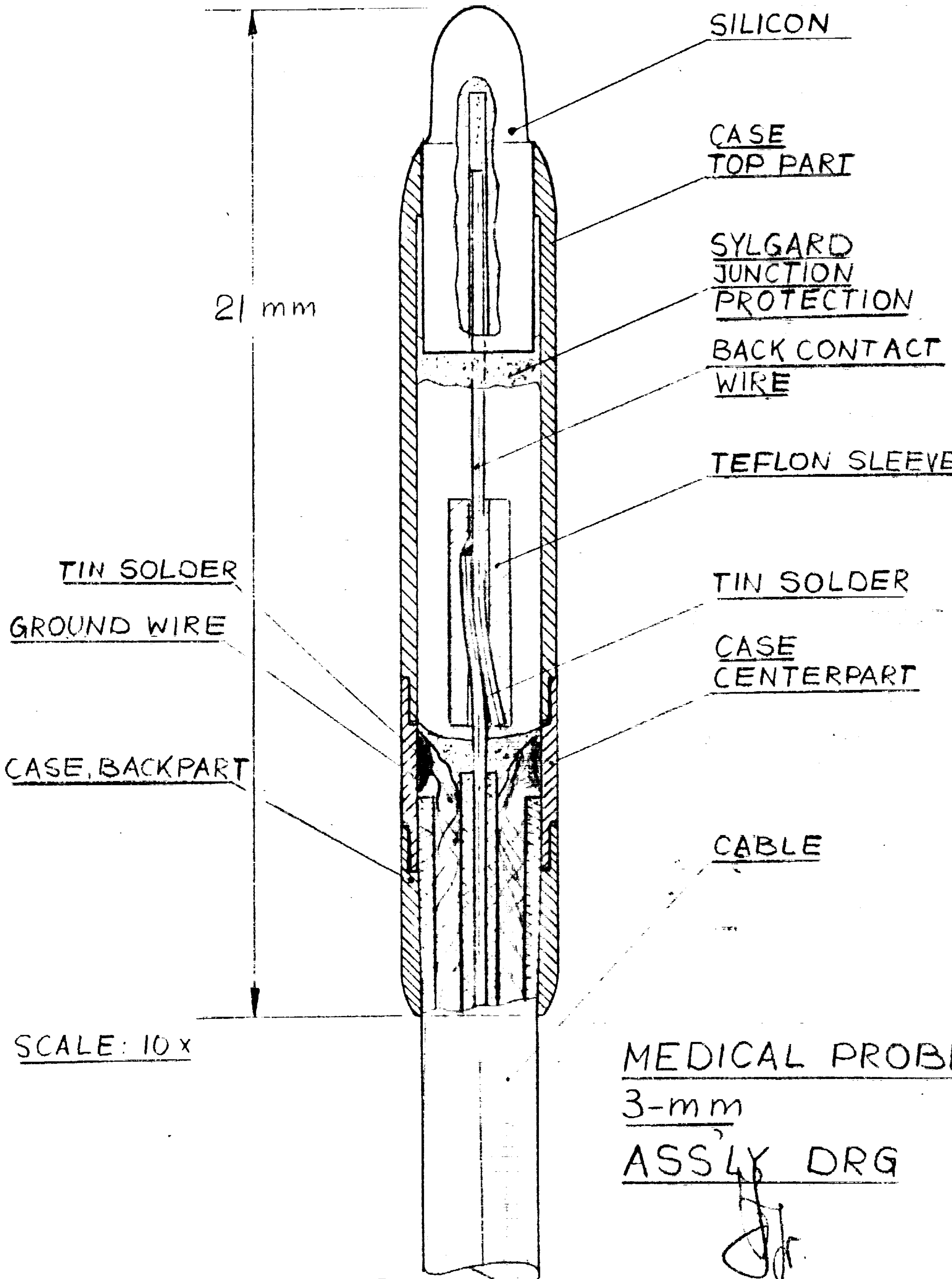

MEDICAL PROBE
3-mm
ASS'LY DRG

FIG. 8

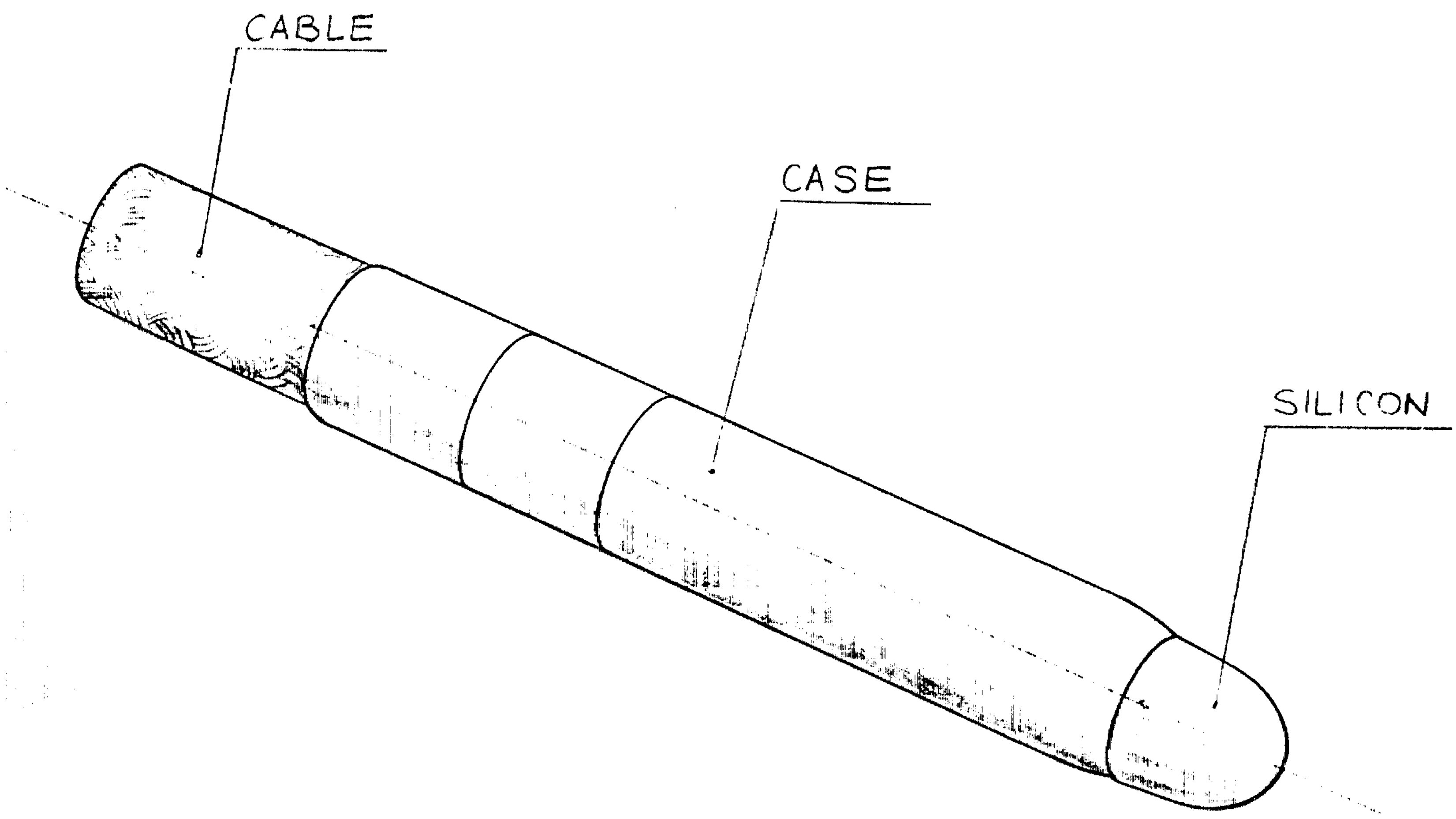

3 mm PROBE

~10 x ENLARGED

FIG. 9

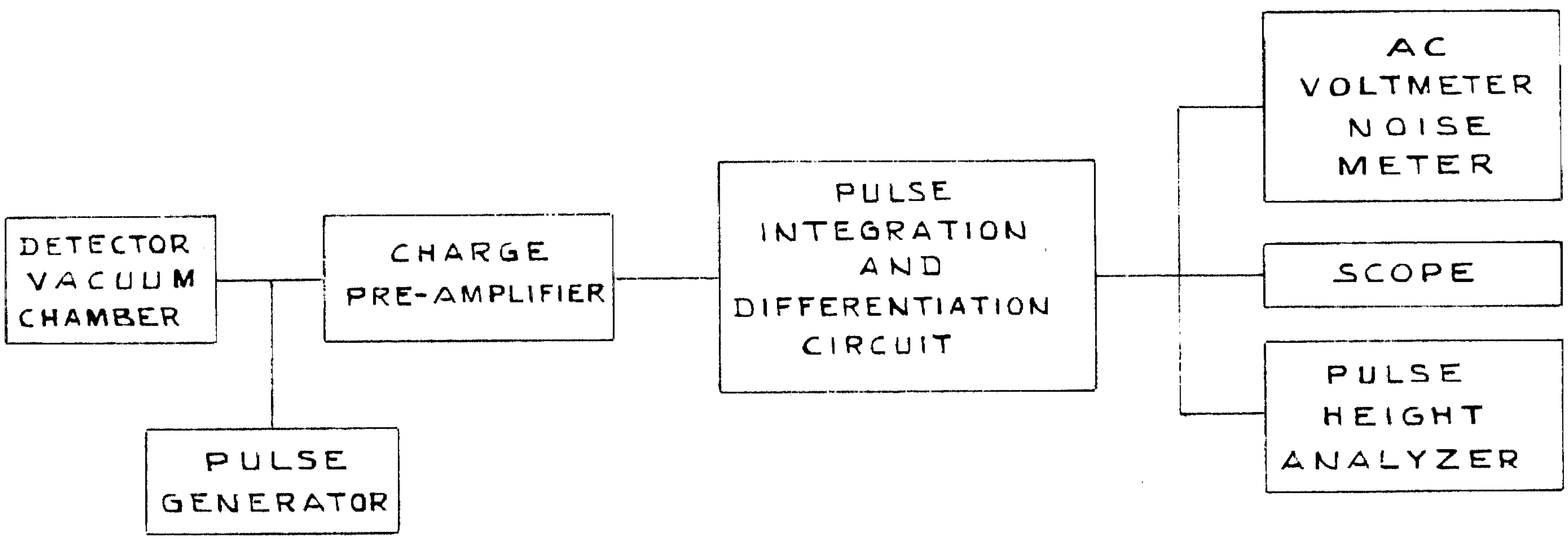

ELECTRONIC SYSTEM FOR SEMICONDUCTOR NUCLEAR PARTICLE DETECTOR EVALUATION

FIG. 10

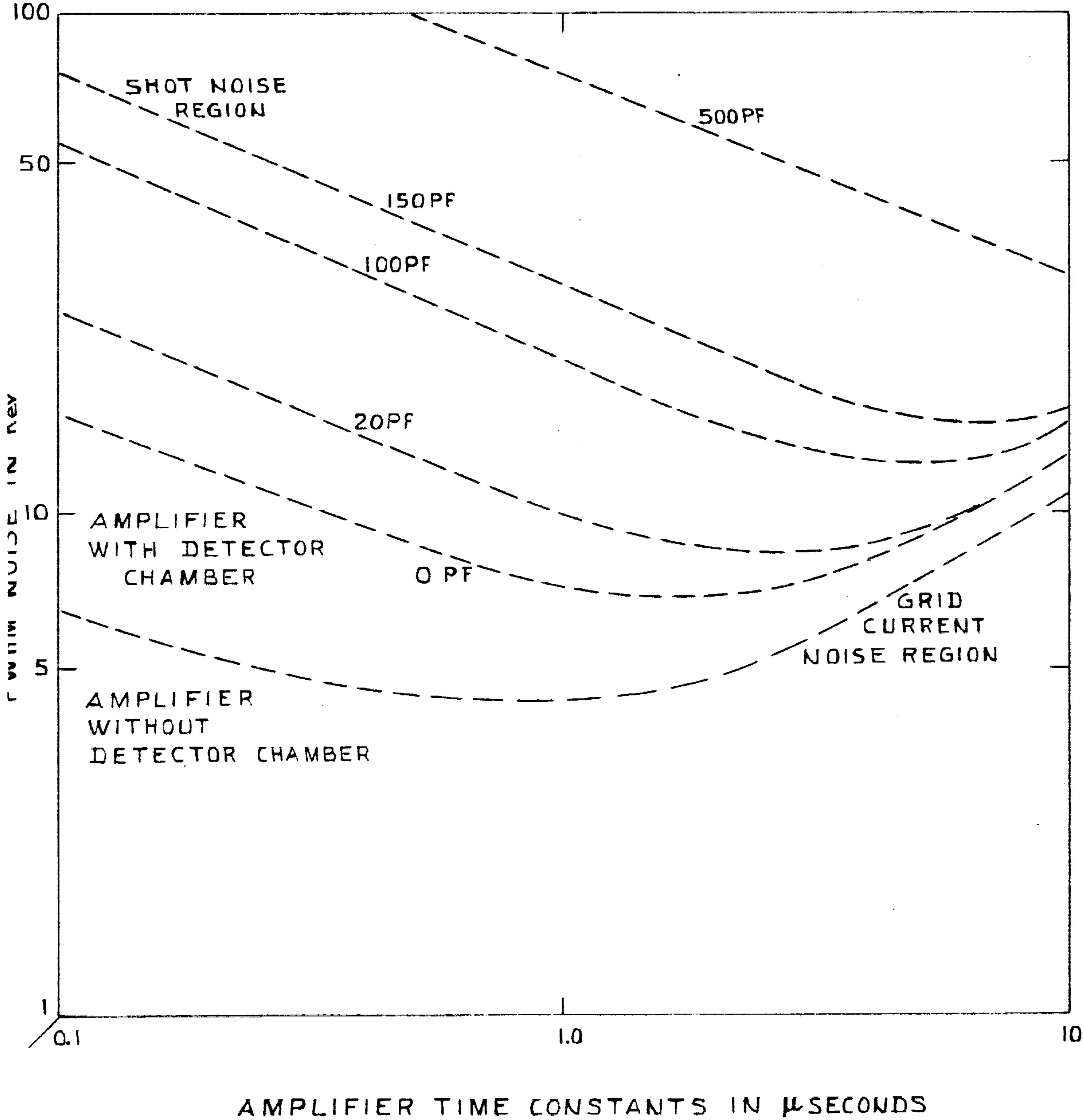

100
50
10
5
1
0.1
1.0
10
SHOT NOISE REGION
500PF
150PF
100PF
20PF
0 PF
AMPLIFIER WITH DETECTOR CHAMBER
AMPLIFIER WITHOUT DETECTOR CHAMBER
GRID CURRENT NOISE REGION
AMPLIFIER TIME CONSTANTS IN μSECONDS

FIG. 11

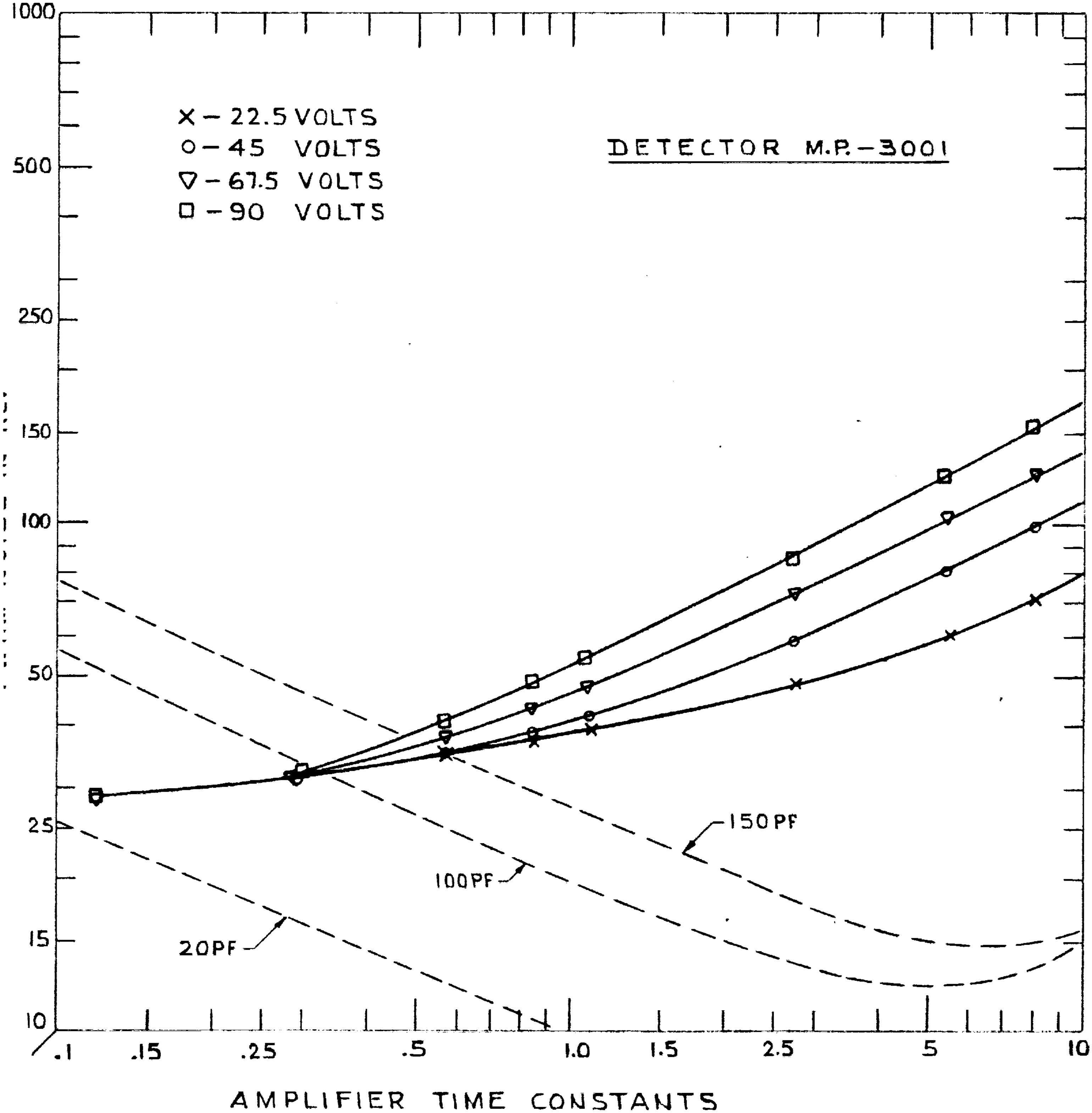
X – 22.5 VOLTS
O – 45 VOLTS
∇ – 67.5 VOLTS
□ – 90 VOLTS
DETECTOR M.P.–3001
1000
500
250
150
100
50
25
15
10
.1
.15
.25
.5
1.0
1.5
2.5
5
10
150 PF
100PF
20PF
AMPLIFIER TIME CONSTANTS

FIG.12

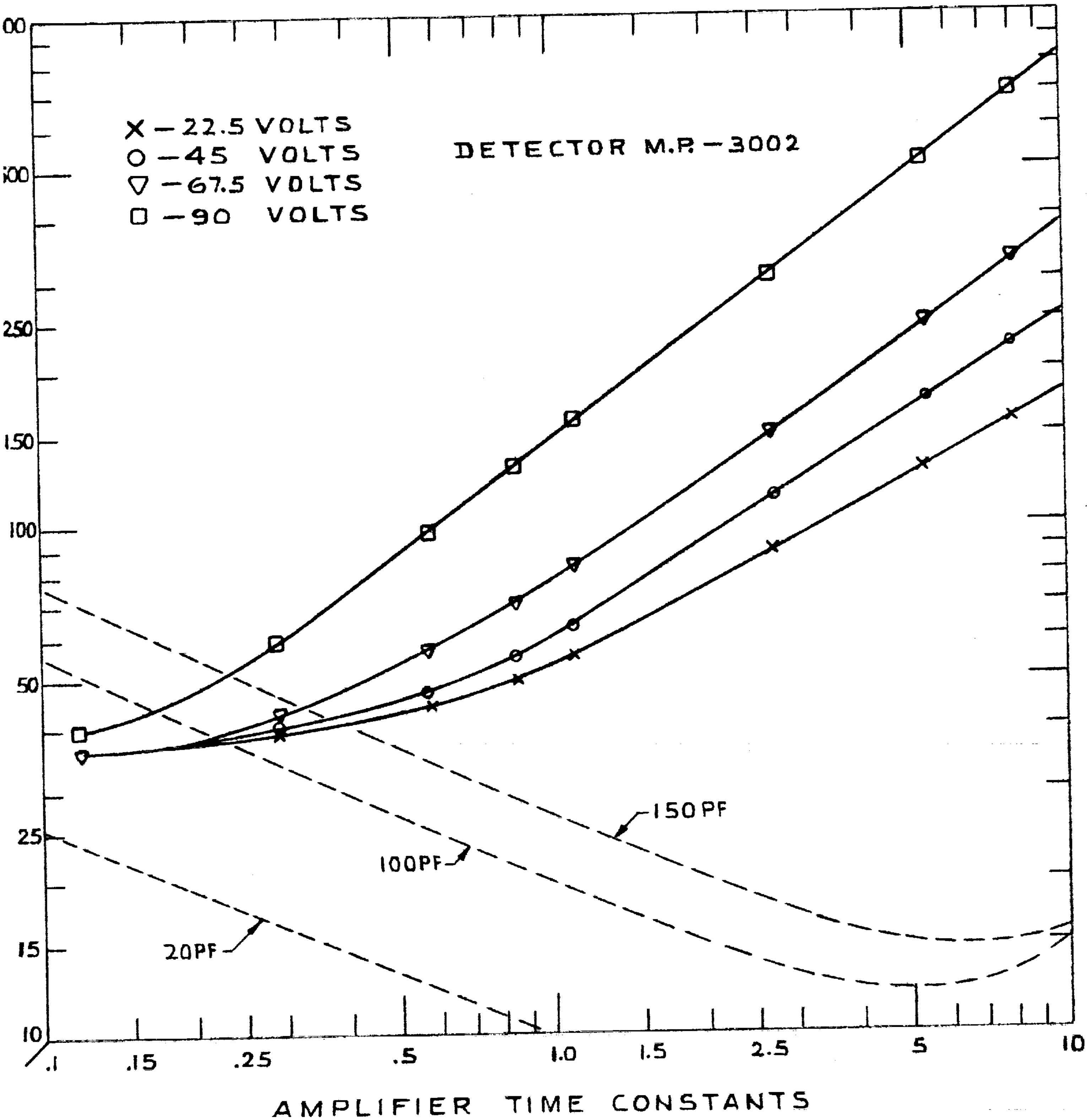
X — 22.5 VOLTS
O — 45 VOLTS
∇ — 67.5 VOLTS
□ — 90 VOLTS
DETECTOR M.P. — 3002
150PF
100PF
20PF
10
15
25
50
100
150
250
.1
.15
.25
.5
1.0
1.5
2.5
5
10
AMPLIFIER TIME CONSTANTS

FIG. 13

ALPHA SPECTRUM
SIDE OF DETECTOR

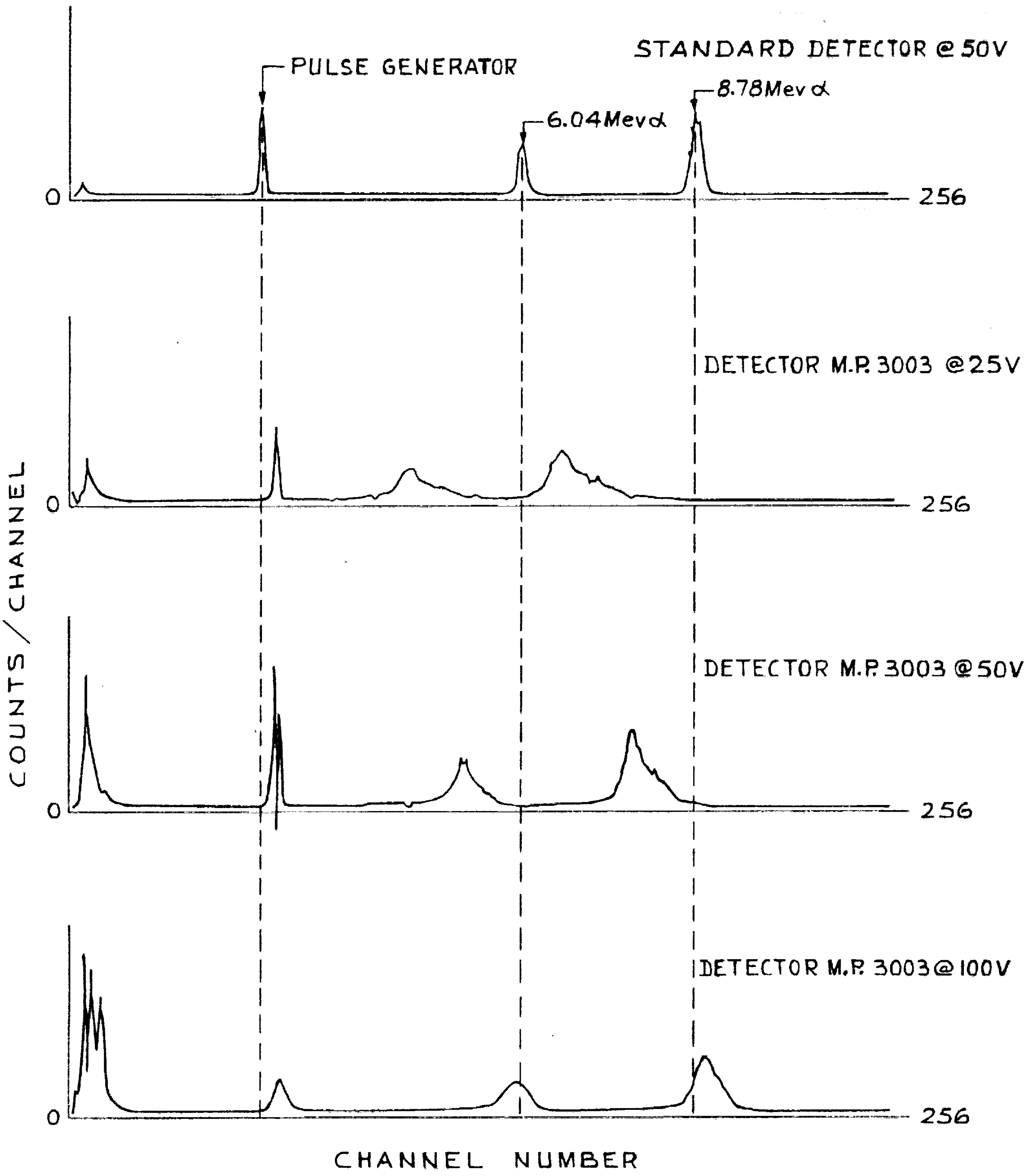

FIG. 14

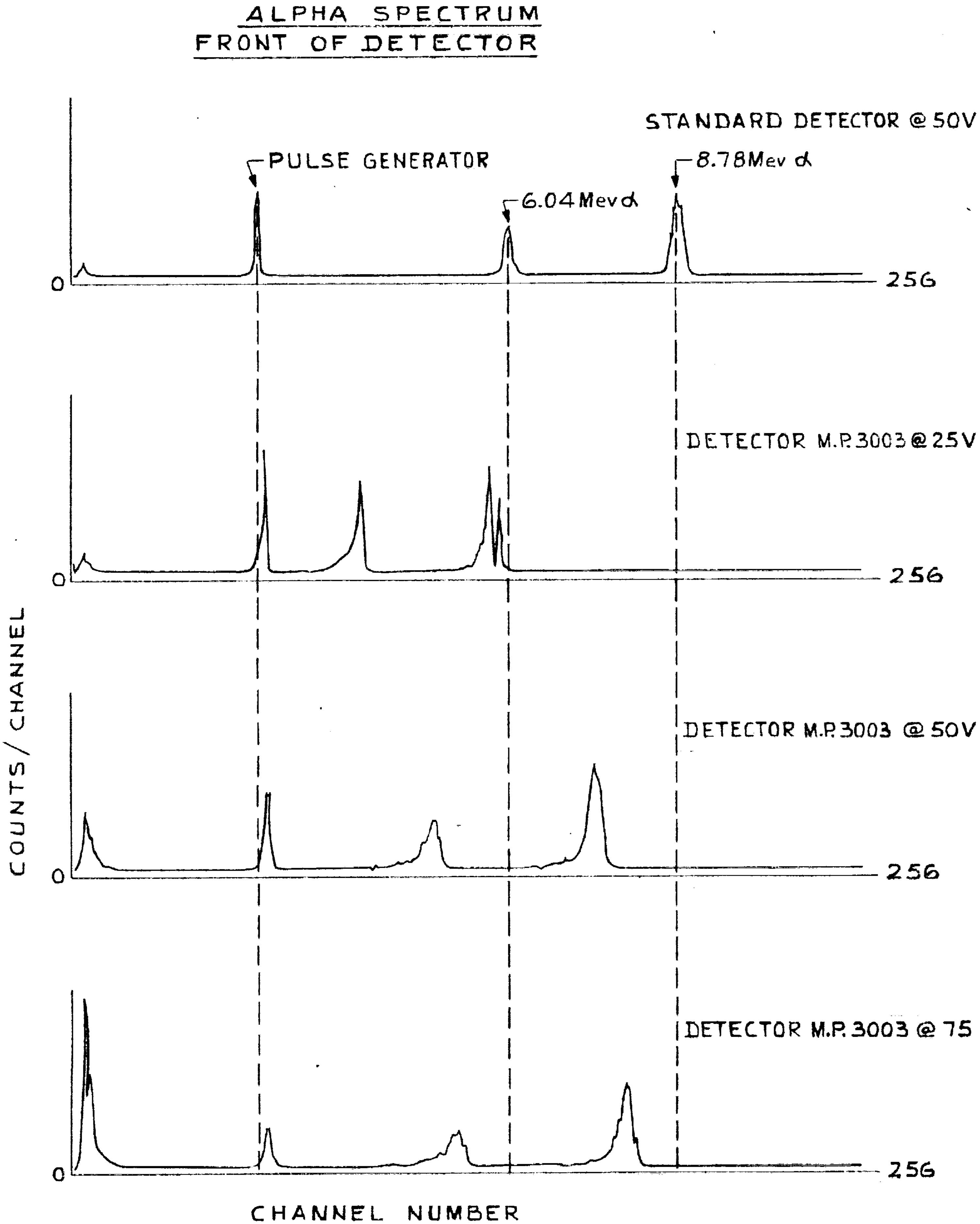
ALPHA SPECTRUM
FRONT OF DETECTOR
STANDARD DETECTOR @ 50V
PULSE GENERATOR
6.04 Mev α
8.78 Mev α
DETECTOR M.P. 3003 @ 25V
DETECTOR M.P. 3003 @ 50V
DETECTOR M.P. 3003 @ 75
0
256
COUNTS / CHANNEL
CHANNEL NUMBER

FIG. 15

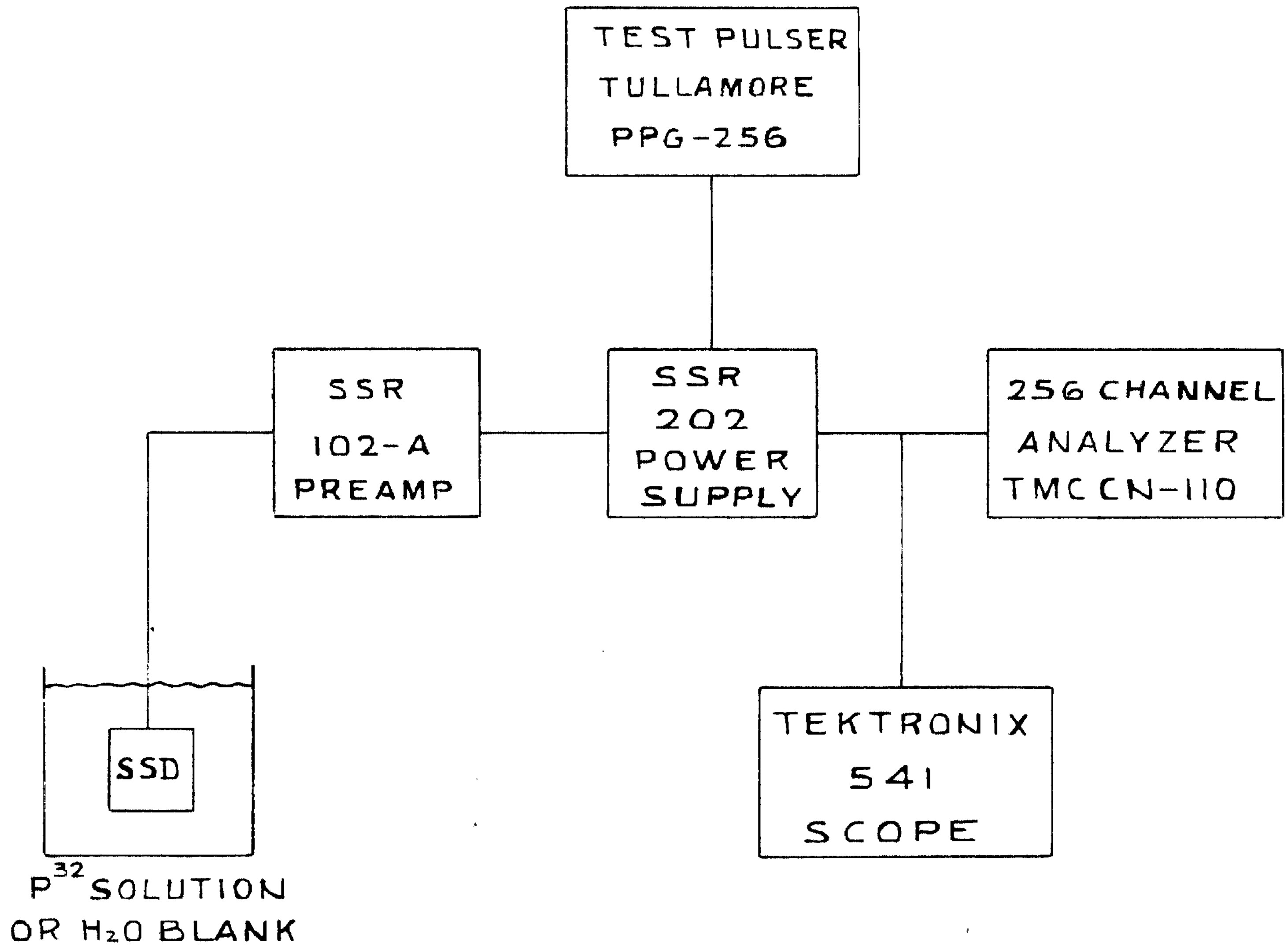

BLOCK DIAGRAM OF P^{32} IRRADIATION OF MEDICAL PROBE DETECTOR MEASUREMENTS

FIG. 16